Chinese Chemical Letters 36 (2025) 109876

Contents lists available at ScienceDirect

Chinese Chemical Letters

journal homepage: www.elsevier.com/locate/cclet

Accurate visualization colorectal cancer by monitoring viscosity variations with a novel mitochondria-targeted fluorescent probe

Fan Zheng[a,b,1], Runsha Xiao[c,d,e,1], Shuai Huang[a,b], Zhikang Chen[c,d,e], Chen Lai[c,d,e], Anyao Bi[a,b], Heying Yao[a,b], Xueping Feng[e,f,g], Zihua Chen[c,d,e,*], Wenbin Zeng[a,b,*]

[a] Xiangya School of Pharmaceutical Sciences, Central South University, Changsha 410013, China
[b] Hunan Key Laboratory of Diagnostic and Therapeutic Drug Research for Chronic Diseases, Central South University, Changsha 410013, China
[c] Department of General Surgery, Xiangya Hospital, Central South University, Changsha 410008, China
[d] Hunan Key Laboratory of Precise Diagnosis and Treatment of Gastrointestinal Tumor, Xiangya Hospital, Central South University, Changsha 410008, China
[e] National Clinical Research Center for Geriatric Disorders, Xiangya Hospital, Central South University, Changsha 410008, China
[f] Department of Oncology, Xiangya Hospital, Central South University, Changsha 410008, China
[g] Department of Otolaryngology-head and Neck Surgery and Institute of Medical Sciences, Xiangya Hospital, Central South University, Changsha 410008, China

ARTICLE INFO

Article history:
Received 13 February 2024
Revised 2 April 2024
Accepted 8 April 2024
Available online 9 April 2024

Keywords:
Fluorescent probe
Viscosity
Bioimaging
Colorectal cancer
Cancer diagnosis
Mitochondrial-targeted

ABSTRACT

Colorectal cancer (CRC) is one of the most prevalent malignant tumors worldwide, exhibiting high morbidity and mortality. Lack of efficient tools for early diagnosis and surgical resection guidance of CRC have been a serious threat to the long-term survival rate of the CRC patients. Recent studies have shown that relative higher viscosity was presented in tumor cells compared to that in normal cells, leading to viscosity as a potential biomarker for CRC. Herein, we reported the development of a series of novel viscosity-sensitive and mitochondria-specific fluorescent probes (**HTB**, **HTI**, and **HTP**) for CRC detection. Among them, **HTB** showed high sensitivity, minimal background interference, low cytotoxicity, and significant viscous response capability, making it an ideal tool for distinguishing colorectal tumor cells from normal cells. Importantly, we have successfully utilized **HTB** to visualize in a CRC-cells-derived xenograft (CDX) model, enriching its medical imaging capacity, which laid a foundation for further clinical translational application.

Colorectal cancer (CRC), accounting for over 1.9 million new cases and 0.9 million deaths each year, is the second most common cancer in global prevalence which presents a serious threat to human health [1–3]. Among this, radical resection is an appropriate solution for about 75% of patients with CRC [4,5]. Nevertheless, the low rate of early diagnosis and the high rate of postoperative failure extremely hinders the long-term survival rate of the CRC patients [6]. In this scenario, numerous resources are devoted to advancing imaging technologies to assist early diagnosis and accurate surgical resection. So far, computed tomography (CT), positron emission tomography (PET), and magnetic resonance imaging (MRI) have made great contributions in the diagnosis of CRC [7–9]. However, these imaging modalities generally suffer from radiation, high cost, and low sensitivity [10,11]. Compared with these techniques, fluorescence imaging, providing real-time images with high sensitivity and high resolution, has been widely applied in distinguishing tumor area from normal tissue, further guiding surgical resection [12–14].

Since the abnormal fluctuation in microenvironment might result in the occurrence and progression of cancer, it is of great significance to monitor its alteration to early diagnose cancer [15–17]. Viscosity, as a vital microenvironmental parameter, plays an essential role in transmitting intracellular substances, transporting chemical signals, and affecting biomacromolecular interactions [18,19]. Unusual changes in viscosity could cause malignant growth of cells [20–22]. Meanwhile, relative higher viscosity has been found to be presented in tumor cells than in normal cells due to the accumulation of lactic acid [23]. Thus, developing fluorescent probes for monitoring the fluctuation in viscosity shows great potential in tumor-targeted imaging.

To date, more efforts have been devoted in constructing viscosity-responsive probes to distinguish tumors from normal tissues [24–26]. For example, Li *et al.* reported a xanthene-based

* Corresponding authors.
E-mail addresses: zihuac@outlook.com (Z. Chen), wbzeng@hotmail.com (W. Zeng).
[1] These authors contributed equally to this work.

https://doi.org/10.1016/j.cclet.2024.109876
1001-8417/

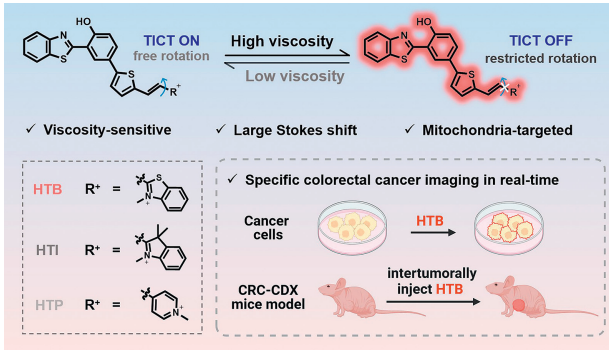

Scheme 1. Schematic illustration of specifically imaging colorectal cancer utilizing a viscosity-sensitive and mitochondria-specific probe **HTB**.

probe which provided a tool for exploring the relationship between viscosity and cancer [25]. Qi *et al.* connected the tetraphenylene-like electron donor unit with the cyano-pyridinium salt electron acceptor part to form a viscosity-dependent probe to specifically illuminate tumor cells [26]. However, these developed probes either suffered from short excitation wavelength or small Stokes shift, which limited their further application in clinic [26,27]. Therefore, designing novel probes to meet these demands can provide safer and lower signal-to-noise ratio imaging for the early clinical diagnosis of tumor-related diseases.

Recently, we had reported a novel mitochondrial viscosity fluorescent probe (**HTI**) to meet this demand which was applied for precise visualization and photodynamic therapy of colorectal cancer [28]. However, its sensitivity towards viscosity, as well as biocompatibility, remained room to improve. Here, we have synthesized two more novel mitochondrial-targeted fluorescent probes (**HTB** and **HTP**) through attaching different electron acceptor units to the fluorophore 2-(2-hydroxyphenyl)benzothiazole (HBT) for sensitive detection of viscosity in CRC. Notably, among these three probes, 2-(2-(5-(3-(benzo[*d*]thiazol-2-yl)−4-hydroxyphenyl)thiophen-2-yl)vinyl)−3-methylbenzo[*d*]thiazol-3-ium iodide (**HTB**) was demonstrated to display the most distinct viscosity-response with the lowest cytotoxicity based on the experimental and calculative data. As illustrated in Scheme 1, **HTB**, with the advantages of its remarkable viscosity sensitivity, minimal background interference, large Stokes shift, and excellent mitochondria-targeted ability, was effectively utilized to distinguish colorectal tumor from normal part based on the difference in mitochondrial viscosity and membrane potential. In a word, **HTB** was deemed as a potential fluorescent probe for precise detecting CRC in real-time.

Generally, a freely rotating group is important in the rational molecular design strategy of viscosity fluorescent probes. Given the intramolecular free rotation, the fluorescence of the probe will be hard to record in the low viscous environment based on the twisted intramolecular charge transfer (TICT) effect. In contrast, the fluorescence will be extremely enhanced in the highly viscous environment since the rotation is restricted. Thus, we introduced different electron acceptor groups to the HBT fluorophore through a freely rotating double bond to obtain probes **HTB**, **HTI**, and **HTP**. The three probes were synthesized in three steps with the C=C bond as recognition site for viscosity (Scheme S1 in Supporting information). Then, we screened out **HTB** with excellent properties by spectral testing and calculation to provide remarkable viscosity-response performance in tumor-specific imaging. The characterization of the chemical structure of these probes was validated by nuclear magnetic resonance imaging (NMR) and high-resolution mass spectrometry (HRMS), as shown in the supporting information (Figs. S8–S16 in Supporting information).

With the probes in hand (Figs. 1A, E and I), the spectral properties were firstly investigated. As illustrated in Fig. S1 (Supporting information), the absorption peaks of **HTB**, **HTI**, and **HTP** were around at 480, 500, and 440 nm. As displayed in Figs. 1B, F and J, the emission peaks of **HTB**, **HTI**, and **HTP** were at around 610, 615, and 585 nm, reflecting large Stokes shifts of 130, 115, and 145 nm, respectively. Furthermore, it is worth noting that strikingly strong fluorescence of these probes was only displayed in glycerin rather than showing in other solvents, implying a capacity of viscosity response. Under this circumstance, the quantitative evaluation of the probes against viscosity was carried out in different methanol/glycerol miscible systems from 1.57 cP (100% methanol) to 2043 cP (100% glycerol). As shown in Figs. 1C, G and K, the fluorescence intensity of the probes remarkably enhanced with the increased fraction of glycerol. More importantly, the emission intensity showed an excellent linear relationship with viscosity (Figs. 1D, H and L). The Förster-Hoffmann equation can typically reflect the values of viscosity sensitivity [22]. Among them, **HTB** displayed the largest slope (0.3607) based on the Förster-Hoffmann equation and the most significant change in the fluorescence intensity from methanol to glycerol (14-fold increase), indicating the highest sensitivity towards viscosity. Then, the interference of other biologically related species towards the probes was explored. With the addition of various cations, anion, reactive oxygen species, or amino acids, the changes in the fluorescence were negligible (Figs. S2A–C in Supporting information). Moreover, few fluctuations in fluorescence were depicted under physiological pH conditions (Figs. S2D–F in Supporting information). Then, time-dependent density functional theory (TDDFT) calculations were performed to reveal the optimized geometry of the probes utilizing Gaussian 16 software (CAM-B3LYP/Def2-svp). The excited state was analyzed by electron-hole analysis. As shown in Fig. S3 (Supporting information), the hole was mainly located on the phenol of HBT and the thiophene part, while electron was mainly located on the positive-charged electron acceptor groups. It reflected that this series of probes had a typical twisting intramolecular charge transfer (TICT) effect. Collectively, these results demonstrated that the three probes were feasible for sensitively and selectively monitoring viscous changes, especially **HTB**.

Based on the fabulous properties of the three probes *in vitro*, we further investigated the intracellular imaging capacity. Firstly, we conducted the biocompatibility assessment in human colon cancer cell line HCT-116 *via* cell counting kit-8 (CCK8) assay. The cell viability of HCT-116 cells proved that the probes were negligible toxic to live cells (Fig. S4 in Supporting information). More importantly, the cell proliferation activity affected by **HTB** was observed to be minimum which maintained over 85% at concentrations up to 30 μmol/L.

Then, a colocalization experiment using confocal laser scanning microscopy (CLSM) was conducted. Since a positive charge was involved in the structure of the probes, it might enable them to target mitochondria through the electrostatic interaction with the mitochondrial membrane [29]. In this scenario, we speculated that the probes could accumulate in mitochondria. Thus, HCT-116 cells were incubated with probes and Mitotracker Rhodamine-123 or Lysotracker Green to evaluate the targeting capacity. As shown in Fig. 2, the fluorescence signals of Rhodamine-123 were vigorously overlapped with that of the probes with a Pearson's colocalization coefficient over 0.9. Comparatively, the Pearson's correlation coefficient between probes and Lysotracker Green was only around 0.4 (Fig. S5 in Supporting information). The results had verified our hypothesis that the probes could predominantly achieve mitochondrial directing.

Inspired by the extraordinary targeting capacity of the probes towards mitochondria, the practicality in monitoring mitochondrial viscosity fluctuations was conducted. As reported, nystatin, a com-

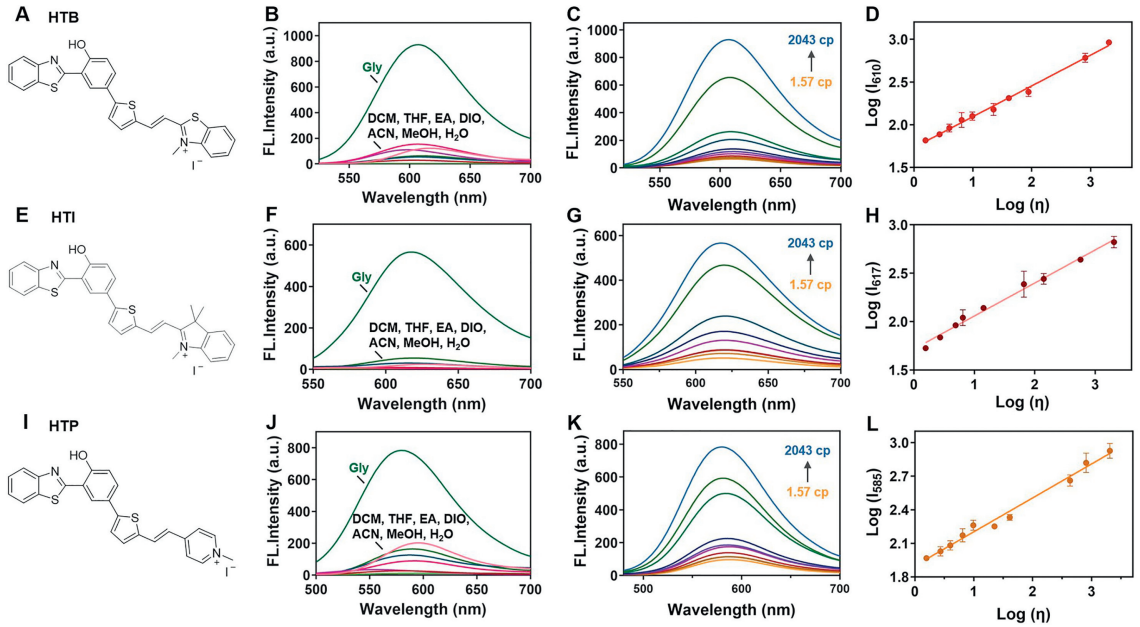

Fig. 1. (A) Chemical structure of **HTB**. (B) Fluorescence spectra of **HTB** (10 μmol/L) in various solvents. (C) Fluorescence spectra of **HTB** (10 μmol/L) in methanol containing an increasing proportion of glycerin. $\lambda_{ex} = 480$ nm. (D) Dependence of Log(I) on Log(η). Log(I_{610}) = 0.3607 × Log(η) + 1.733 ($R^2 = 0.9945$). (E) Chemical structure of **HTI**. (F) Fluorescence spectra of **HTI** (10 μmol/L) in various solvents. (G) Fluorescence spectra of **HTI** (10 μmol/L) in methanol containing an increasing proportion of glycerin. $\lambda_{ex} = 500$ nm. (H) Dependence of Log(I) on Log(η). Log(I_{617}) = 0.3419 × Log(η) + 1.709 ($R^2 = 0.9935$). (I) Chemical structure of **HTP**. (J) Fluorescence spectra of **HTP** (10 μmol/L) in various solvents. (K) Fluorescence spectra of **HTP** (10 μmol/L) in methanol containing an increasing proportion of glycerin. $\lambda_{ex} = 440$ nm. (L) Dependence of Log(I) on Log(η). Log(I_{585}) = 0.3032 × Log(η) + 1.899 ($R^2 = 0.9860$). Data are presented as mean ± standard deviation (SD) ($n = 3$).

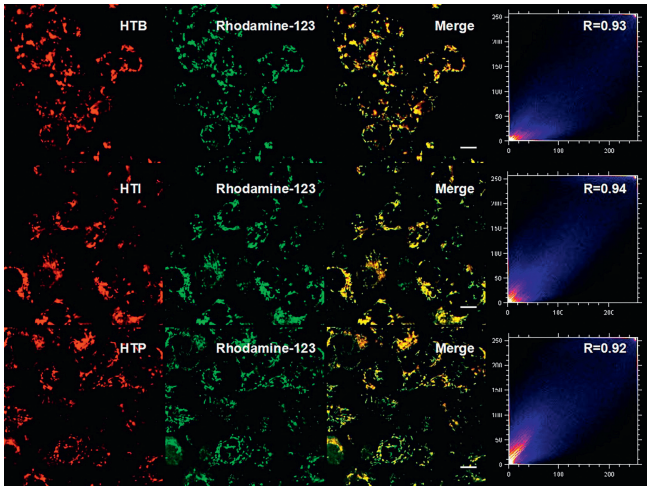

Fig. 2. CLSM images of **HTB**, **HTI**, or **HTP** (10 μmol/L) co-stained with Rhodamine 123 in HCT-116 cells separately. Green channel for Rhodamine 123, $\lambda_{ex} = 488$ nm, $\lambda_{em} = 525 \pm 20$ nm. Red channel for **HTB**: $\lambda_{ex} = 546$ nm, $\lambda_{em} = 610 \pm 20$ nm, **HTI**: $\lambda_{ex} = 568$ nm, $\lambda_{em} = 620 \pm 20$ nm, **HTP**: $\lambda_{ex} = 405$ nm, $\lambda_{em} = 580 \pm 20$ nm. Scale bar: 10 μm.

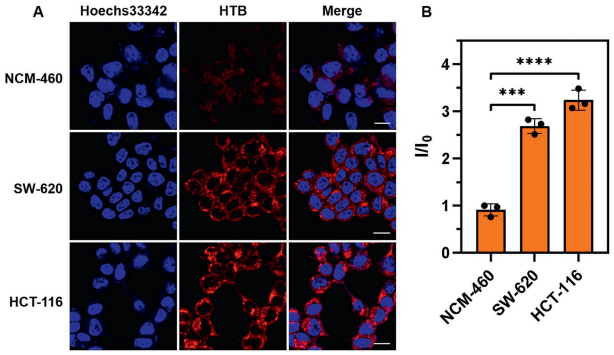

Fig. 3. The capability of **HTB** to distinguish CRC cells from normal cells. (A) Viscosity inspection using **HTB** (10 μmol/L) in epithelial cells (NCM-460) and in different colon cells (SW-620 and HCT-116). Blue channel for Hoechst33342: $\lambda_{ex} = 405$ nm, $\lambda_{em} = 455 \pm 20$ nm. Red channel for **HTB**: $\lambda_{ex} = 546$ nm, $\lambda_{em} = 610 \pm 20$ nm. Scale bar: 10 μm. (B) The plots of relative fluorescence intensities in NCM-460, SW-620, and HCT-116 cells. Data are presented as mean ± SD ($n = 3$). $^{***}P < 0.001$, $^{****}P < 0.0001$.

monly used antifungal drug, can induce mitochondrial dysfunction and cause viscous variation [30]. Prior to the intracellular application of nystatin, no distinct fluorescence changes were recorded after coexisting it with the probes in solution (Fig. S6 in Supporting information). Then, the cells were pretreated with 10 μmol/L probe, followed by incubation with nystatin for different times. As can be seen from Fig. S7 (Supporting information), the red fluorescence of the probes gradually enhanced with the increased incubation time with nystatin, indicating real-time imaging of mitochondrial viscosity by the developed probes. It is worth noting that the most remarkable enhancement in fluorescence towards viscosity was observed utilizing probe **HTB**. Comprehensively considering the results of the spectral properties, the theoretical calculation, and the cells assessments, **HTB** exhibited high sensitivity, low cytotoxicity, and good intracellular imaging capacity to monitor viscous changes, which was selected to be implemented for further biological application.

Based on the urgent need for early screening of tumors, detection means which can efficient discriminate tumor cells will greatly contribute to clinical diagnosis and treatment. In this fields, fluorescent probes perfectly meet this requirement, offering a choice at low cost, high sensitivity, and real-time monitoring [31,32]. Therefore, **HTB** was applied in tumor cell discrimination based on its ability to inspecting mitochondrial viscosity. As shown in Fig. 3, significant red signals of **HTB** were captured in the colon cancer cells compared to that in the normal colon epithelial cells. This result indicated that **HTB** was capable of distinguishing tumor

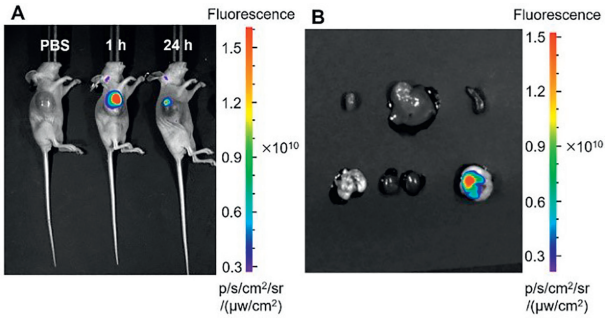

Fig. 4. The capability of **HTB** to label tumor in CRC–CDX mice model. (A) *In vivo* fluorescence image of **HTB** (100 μmol/L, 100 μL) labelled tumor after the intertumoral injection at different time points. (B) Comparation of tumor *versus* normal organs (heart, liver, spleen, lung, and kidney) 1 h after intertumoral injection of **HTB**.

cells from normal cells in view of the distinction of mitochondrial viscosity with high spatiotemporal resolution, providing an innovative tool for clinical practice to improve the early detection rate of CRC.

Profit by the exceptional characteristics of **HTB** *in vitro*, we decided to continue the assessment *in vivo*. Cells-derived xenograft (CDX) model was established using HCT-116 cells in BALB/c nude mice. All animal experiments were performed according to the relevant ethical regulations of Xiangya Hospital, and this study received approval from Experimental Animal Ethics Committee of Xiangya Hospital, Central South University. HCT-116 cells at a density of 1×10^7/mL were subcutaneously inoculated in right forelimb armpit of mice 100 μL each. After the tumor grew up to approximately 800 mm^3 under specific pathogen-free conditions, mice were used to serve as a colorectal cancer CDX model. **HTB** (100 μmol/L, 100 μL) was previously intratumorally injected in tumor region on mice, then, *in vivo* fluorescence images were captured at the time point of 1 and 24 h. The bio-compatibility and metabolic stability of **HTB** were depicted in Fig. 4A. High intensity signal, due to the high viscosity environment in tumor site, was clearly captured 1 h after the injection of **HTB** compared to the phosphate-buffered saline (PBS) group. And bright fluorescence signal could still be maintained in the tumor region even after 24 h. Mice were euthanized after imaging, then main normal organs (heart, liver, spleen, lung, and kidney) and tumor were isolated for *ex vivo* fluorescence imaging (Fig. 4B). Distinct fluorescence signal was only observed on tumor which demonstrated the retention effect and the specificity of **HTB** *in vivo*. These performances duly indicated that **HTB** was a feasible and efficient real-time fluorescent probe with tumor retention capability, further possessing clinical translational application prospects.

In summary, this study proposed the development of a series of HBT-based fluorescent probes to evaluate for an efficient tool for real-time and accurate diagnose CRC. It was demonstrated that **HTB** exhibited large Stokes shift, as well as high viscous sensitivity and selectivity. With its excellent physicochemical properties, **HTB** could qualitatively and quantitatively detect mitochondrial viscosity changes. Then, **HTB** was utilized to distinguish colorectal cells from normal cells based on the difference in mitochondrial viscosity and membrane potential. In addition, the imaging capacity of the probe was validated *in vivo*. Collectively, this work has provided a potential tool for early CRC diagnosis and its versatility held great promise for studying other viscosity abnormal-related diseases.

Declaration of competing interest

The authors declare that they have no known competing financial interests or personal relationships that could have appeared to influence the work reported in this paper.

CRediT authorship contribution statement

Fan Zheng: Writing – original draft, Methodology, Investigation, Formal analysis, Data curation. **Runsha Xiao:** Writing – original draft, Methodology, Investigation, Formal analysis, Data curation. **Shuai Huang:** Methodology, Investigation, Data curation. **Zhikang Chen:** Methodology, Data curation. **Chen Lai:** Investigation, Data curation. **Anyao Bi:** Methodology, Conceptualization. **Heying Yao:** Formal analysis, Data curation. **Xueping Feng:** Resources, Project administration, Investigation. **Zihua Chen:** Supervision, Resources, Project administration, Conceptualization. **Wenbin Zeng:** Writing – review & editing, Supervision, Resources, Project administration, Conceptualization.

Acknowledgments

This work was supported by the National Natural Science Foundation of China (Nos. 82272067, 81974386, M-0696, and 82273486), Natural Science Foundation of Hunan Province (Nos. 2022JJ80052, 2024JJ6596), and the Innovation Fund for Postgraduate Students of Central South University (No. 2023ZZTS0841).

Supplementary materials

Supplementary material associated with this article can be found, in the online version, at doi:10.1016/j.cclet.2024.109876.

References

[1] H. Sung, J. Ferlay, R.L. Siegel, et al., CA Cancer J. Clin. 71 (2021) 209–249.
[2] Y. Xi, P. Xu, Transl. Oncol. 14 (2021) 101174.
[3] W. Chen, K. Shi, Y. Yu, et al., Chin. Chem. Lett. 35 (2024) 109159.
[4] X. Liang, M. Mu, B. Chen, et al., Mater. Today Adv. 16 (2022) 100308.
[5] S. Zha, T. Li, Q. Zheng, L. Li, Front. Pharmacol. 13 (2022) 826785.
[6] Y. Wu, H. Cao, S. Yang, C. Liu, Z. Han, Heliyon 9 (2023) 23209.
[7] C. Shangguan, C. Yang, Z. Shi, et al., Int. J. Radiat. Oncol. Biol. Phys. 118 (2024) 285–294.
[8] B. Gorgec, I.S. Hansen, G. Kemmerich, et al., Lancet Oncol. 25 (2024) 137–146.
[9] X. Li, J. Niu, L. Deng, et al., Acta Biomater. 73 (2024) 432–441.
[10] F. Zheng, X. Huang, J. Ding, et al., Front. Chem. 10 (2022) 859948.
[11] Y. Wang, Y. Hu, D. Ye, Angew. Chem. Int. Ed. 61 (2022) 202209512.
[12] J. Wu, A. Bi, F. Zheng, et al., Chem. Commun. 57 (2021) 801–804.
[13] S. Ma, B. Sun, M. Li, et al., J. Nanobiotechnol. 21 (2023) 403.
[14] R. Pal, T.M. Lwin, M. Krishnamoorthy, et al., Nat. Biomed. Eng. 7 (2023) 1649–1666.
[15] Y. Wang, L. Fu, Y. Tan, Y. Ding, W. Qing, Anal. Bioanal. Chem. 416 (2024) 341–348.
[16] S. Zeng, Y. Wang, C. Chen, et al., Angew. Chem. Int. Ed. 63 (2024) e202316487.
[17] L. Lian, R. Zhang, S. Guo, et al., Chin. Chem. Lett. 34 (2023) 108516.
[18] X. Yang, D. Zhang, Y. Ye, Y. Zhao, Coord. Chem. Rev. 453 (2022) 214336.
[19] M.K. Kuimova, S.W. Botchway, A.W. Parker, et al., Nat. Chem. 1 (2009) 69–73.
[20] H.J. Halpern, G.V.R. Chandramouli, E.D. Barth, et al., Cancer Res. 59 (1999) 5836–5841.
[21] H. Wang, Y. Sun, X. Lin, et al., Chin. Chem. Lett. 34 (2023) 107626.
[22] D. Li, T. Shen, X. Xue, et al., Sci. China Chem. 66 (2023) 2329–2338.
[23] S. Wang, W.X. Ren, J.T. Hou, et al., Chem. Soc. Rev. 50 (2021) 8887–8902.
[24] W. Wang, Y. Liu, J. Niu, W. Lin, Analyst 144 (2019) 6247–6253.
[25] J.J. Chao, H. Zhang, Z.Q. Wang, et al., Anal. Chim. Acta 1285 (2024) 342024.
[26] J. Deng, X. Wang, Y. Zhao, et al., Spectrochim. Acta Part A 305 (2024) 123503.
[27] J. Yu, S. Yuan, K. Sun, et al., Spectrochim. Acta Part A 308 (2024) 123714.
[28] R. Xiao, F. Zheng, K. Kang, et al., Biomater. Res. 27 (2023) 112.
[29] Y. Wu, C. Yin, W. Zhang, Y. Zhang, F. Huo, Anal. Chem. 94 (2022) 5069–5074.
[30] M.R. Clark, J.C. Guatelli, A.T. White, S.B. Shohet, Biochim. Biophys. Acta 646 (1981) 422–432.
[31] S. Park, E. Cho, S.T.D. Chueng, et al., Biosensors 13 (2023) 617.
[32] S.M. Usama, B. Zhao, K. Burgess, Chem. Soc. Rev. 50 (2021) 9794–9816.